

X-Ray Computer Tomography – Potential and Limitation for the Measurement of Local Solids Distribution in Circulating Fluidized Beds

T. Grassler and K.-E. Wirth

Lehrstuhl fuer Mechanische Verfahrenstechnik
Universitaet Erlangen-Nuernberg
Cauerstrasse 4, 91058 Erlangen/GERMANY
Phone: *49-9131-8529400, E-Mail: sekretariat@mvt.uni-erlangen.de

Abstract – *The characterization of the gas-solids flow inside a circulating fluidized bed, especially the knowledge about the solids distribution in the vertical tubes, is the basis for a optimum reactor design as well as for finding suitable operating conditions and for modeling the multiphase flow inside the reactor. To determine data of solids concentration with high spatial resolution an x-ray computer tomography system is used. This system mainly consists of a 60 keV x-ray source and an x-ray linear detector with 1024 sensitive elements, which gives 8 bit-values representing integral solids concentrations between the x-ray source and the detector. A number of experiments have been carried out both at the upflow and at the downflow of two different circulating fluidized beds containing glass beads of 70 μm at superficial gas velocities from 2 to 7 m/s. Results show that the x-ray computer tomography system is applicable to average solids concentrations from 1 up to 20 Vol-% of solids concentration in a tube with 0.19 m inner diameter.*

Keywords: x-ray, computer tomography, circulating fluidized bed, multiphase flow

1. INTRODUCTION

In chemical and process industry vertical multiphase flows play an important role in different fields from processing chemicals and fuel to the production of pharmaceuticals, food and a lot of specialty materials. The characterization of the multiphase flow inside such reactors, especially the knowledge about the concentration distribution in the vertical tube, is the basis for technical constructions.

In the field of process engineering a trend towards simulation and calculation of fluid dynamics and heat transfer can be observed. Such models require accurate data with high spatial resolution, which cannot be obtained by most of the commonly used measurement techniques. In most of the studies, concerned with characterizing flow patterns in circulating fluidized beds, concentration distributions are calculated from vertical pressure gradients or measured with various kinds of intrusive probes [1,2,3]. However, pressure drop profiles only lead to integral values of concentration along a certain length of the tube, if acceleration and deceleration effects are neglected. By using probes a disturbance of the gas-solids flow can never be excluded and often a large-scale calibration is necessary. Moreover, the spatial resolution of probes is poor and only single points of the whole measuring area can be detected at a certain time.

Therefore an x-ray computer tomography system has been developed as a non-intrusive tech-

nique with high spatial resolution to determine the local solids concentration in the tube cross-section of vertical tubes used in pneumatic conveying or circulating fluidized beds.

Tomographic measurements have been carried out at different elevations of two cold-running circulating fluidized beds in a technical scale, both at the upflow and at the downflow. Results from the circulating fluidized beds together with measurements of well defined objects made of plexiglas show the potential and the limits of such a tomographic system in process engineering.

2. PRINCIPLE OF X-RAY COMPUTER TOMOGRAPHY

Computer tomography is a technology, that allows the non-destructive evaluation of the internal structure of objects. Since a lot of years this technique has been used successfully in medicine and material testing to examine local differences in density by generating images of different cutting planes of the object concerned. Recently some efforts have been made to use γ -ray and x-ray computer tomography in multiphase flows [4,5].

Computer tomography systems consist of two main parts, namely a physical measuring technique, which yields to integral values of the wanted local variable along certain paths, and a mathematical reconstruction algorithm, which calculates the local concentrations from the

obtained raw data. In literature a lot of physical sensing methods, available for tomographic measurements, and as well a great number of possible reconstruction techniques can be found [6]. The physical measuring system to obtain the distributions of local solids concentration presented in this paper consists of an x-ray source and an x-ray linear detector to measure the attenuation along a multitude of ray paths through the sample. These data are reconstructed by an Algebraic Reconstruction Technique (ART) [7,8], which is the most common algorithm for industrial applications with limited measurement information.

2.1. Energy spectrum of x-rays

X-rays for technical purposes are normally produced in an x-ray tube. Electrons emitted from a cathode which is heated by a filament are accelerated toward the anode by high voltage between the two electrodes. When the electrons hit the anode, designated as target, they are decelerated which is accompanied by emission of electromagnetic radiation. The emission spectrum of an x-ray tube consists of a continuous spectrum and a characteristic line spectrum.

Wavelength characteristics of the resulting continuous spectrum are completely independent of the target material and depend only on the voltage V_0 applied to the x-ray tube [9]. The higher the voltage, the shorter the minimum or cutoff wavelength produced (see Figure 1). The cutoff wavelength λ_0 can be calculated by the following empirical equation, where h is the Planck's constant, c the velocity of light and e represents the electronic charge:

$$\lambda_0 = \frac{h \cdot c}{e \cdot V_0}$$

with $\frac{h \cdot c}{e} = 1.24 \cdot 10^{-6} \text{ m} \cdot \text{V}$ (1)

The spectral intensity distribution I of the electromagnetic radiation as a function of the wavelength λ can be approximately calculated from [10]:

$$I(\lambda) = \frac{\lambda - \lambda_0}{\lambda^3 \cdot \lambda_0} \quad (2)$$

Equation 2 gives the spectral intensity in any dimensions and represents only the shape of the continuous spectrum.

In addition to that continuous spectrum sharp lines occur in the x-ray region of the spectrum. These lines are superimposed on the continuous x-ray spectrum and can be explained on the basis of the simple Bohr theory. In the target electrons can be removed from the atom by electron collision processes. Then electrons from outer shells can fall into the gap which produces characteristic radiation. This process is strongly

influenced by the pattern of the electron sheath and therefore by the material of the target. The addition of the continuous spectrum and the characteristic line spectrum to the whole x-ray spectrum is shown in Figure 1 on principle.

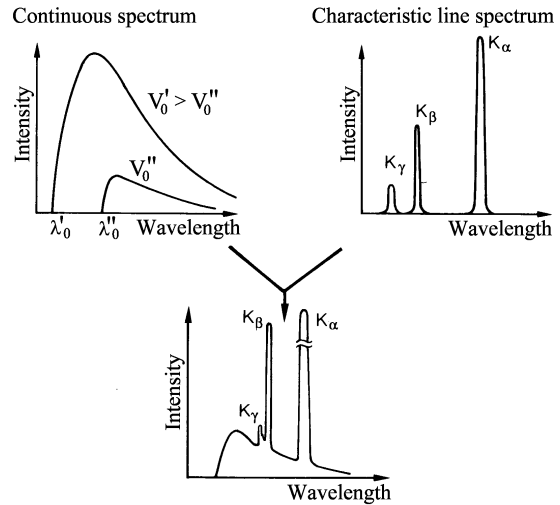


Figure 1: Schematic emissions spectrum of an x-ray source [11]

2.2. Interaction of x-rays with material

If x-rays pass through an object, the original spectral intensity distribution is influenced, depending on the material and the thickness of the object. The irradiation of an infinitesimal thin layer of material ds with a monoenergetic parallel beam causes a decrease in the intensity dI of the radiation, which depends on the linear absorption coefficient of the material μ :

$$dI = -I \cdot \mu \cdot ds \quad (3)$$

With integrating over the whole thickness L of the object the residual intensity I of an original intensity I_0 can be calculated:

$$I = I_0 \cdot e^{-\mu \cdot L} \quad (4)$$

In practice, the linear absorption coefficient μ is no matter constant, but depends on the spectral intensity distribution of the radiation source, the density ρ and the atomic number Z of the object. The reason for the decrease in intensity of the x-ray by penetrating material are three different effects: photoelectric effect, scattering (coherent, incoherent), pair production [12].

- Photoelectric effect and Auger effect: An x-ray quantum hits an electron of the electronic sheath with enough energy to remove this electron. The atom returns to a state of lower energy by filling the hole with an electron from an outer shell and by simultaneously emitting an electromagnetic quantum. If this quantum hits an electron in an outer shell so that the electron is removed, the process is called Auger effect.

- Coherent scattering: When a beam of x-rays passes an electron of the electronic shell, part of

it is scattered into a spherical wave diverging from the location of the electron. X-ray quanta are diffracted from their original direction with retention of their energy.

- Incoherent scattering or Compton effect: When a relatively hard x-ray quantum is scattered by an electron, it partially loses energy to the scattering electron.

- Pair production: If the energy of a quantum is greater than 1.022 MeV, it may be absorbed in the field of an atomic nucleus with the creation or generation of an electron-positron pair. The quantum energy is partly converted into the rest energy of the two created particles, the excess going into their kinetic energy.

The linear absorption coefficient μ can be calculated by adding the extinction coefficients of the different processes of attenuation described above. Figure 2 shows these linear absorption coefficients divided by the material density for the above mentioned effects of attenuation and the total attenuation coefficient in dependence of the x-ray energy E for glass beads (SiO_2), which are used in the experiments.

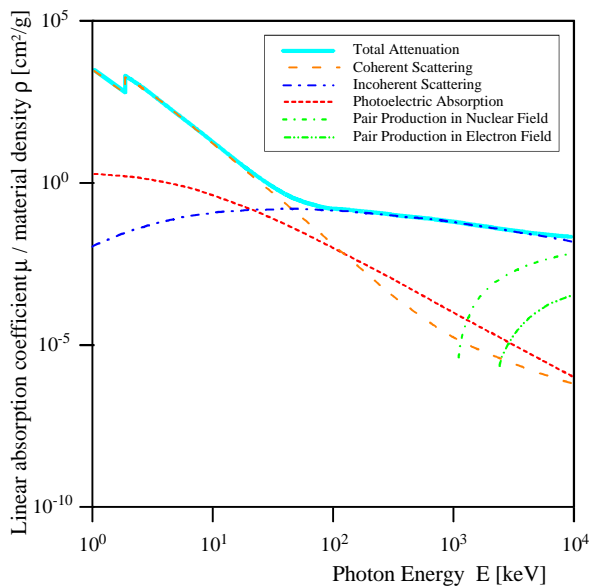


Figure 2: Processes of attenuation in dependence on x-ray energy E for glass beads [13]

For the installed x-ray source with a maximum energy of 60 keV and glass beads that are irradiated, the main processes of attenuation are the photoelectric effect and coherent and incoherent scattering.

The different effects of x-ray absorption cause, that radiation with lower energy is attenuated better than quanta with higher energy. This leads to a shift of the spectral intensity distribution, if material of different thickness is irradiated. This effect of beam hardening is shown in Figure 3, where different layers of aluminum are penetrated by x-rays. This example shows, that

transmissions measurements with x-rays have to be calibrated.

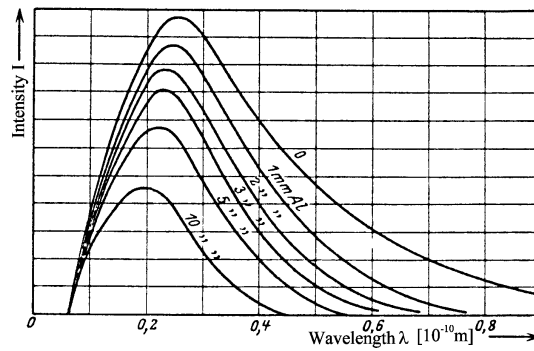


Figure 3: X-ray hardening caused by different layers of aluminum [10]

2.3. Tomographic measuring equipment

The x-ray computer tomography system used mainly consists of a 60 keV x-ray source with an angle of illumination of about 35° and an x-ray linear detector with 1024 sensitive elements and signal resolution of 8 bit. Both components are mounted on a stainless steel ring, which is rotated with the support of a step-by-step motor. Figure 4 shows a scheme of the tomographic system that has been applied to the two different circulating fluidized beds.

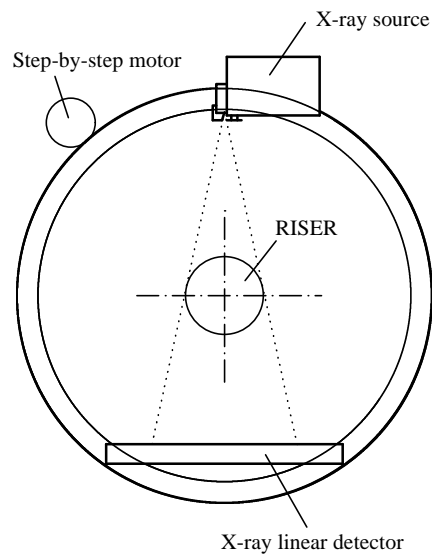


Figure 4: Scheme of the x-ray computer tomography system

The principle of transmission tomography measurements with a radiation source producing a fan beam is pictured in Figure 5. The tube of the circulating fluidized bed is irradiated by fan beams from two different directions in one particular plane. The values of transmission I_1 and I_2 represent the integral value of solids concentration along the approximately linear x-ray beams measured by each of the sensitive

elements of the linear detector. Solids inside the reactor causes additional attenuation in comparison to the empty tube and the values of transmission decrease, which is shown for a simple particle in Figure 5.

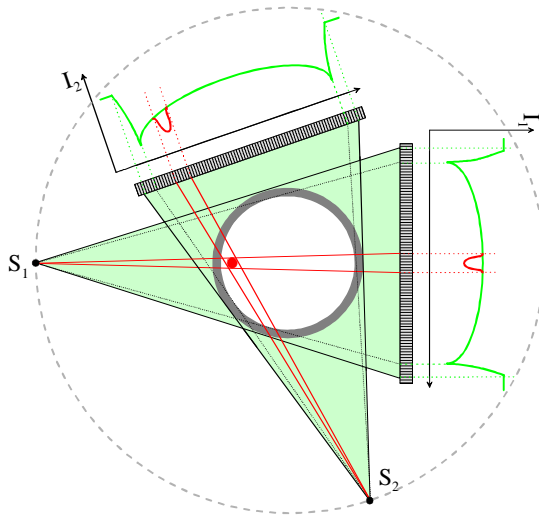


Figure 5: Principle of tomographic measurements

Each of approximately linear x-ray beams is following Beer's Law (Equation 5). So it is possible to calculate the average solids concentration $(1-\epsilon)$ along one path of the x-ray beam s from measured values of transmission with and without a gas-solids flow inside the tube, respectively I and I_0 :

$$(1-\epsilon) = \frac{1}{\int \mu(s) ds} \cdot \ln \frac{I_0}{I} \quad (5)$$

The attenuation due to the gas can be neglected in comparison to the solids. As shown above, the linear absorption coefficient μ is influenced by a number of different variables and therefore it is a function of the beam coordinate s . To calculate average solids concentration according to Equation 5, a calibration for the whole system is necessary.

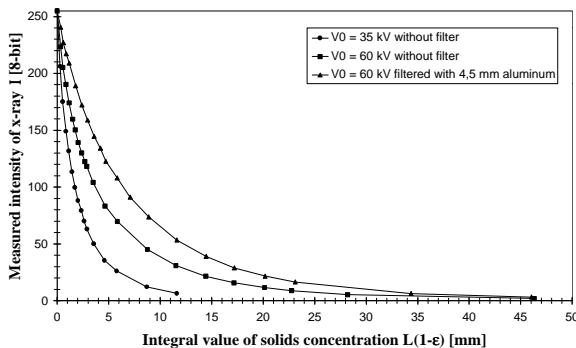


Fig. 6: Calibration of the x-ray computer tomography system

Figure 6 shows measured intensities of the linear detector I for different integral values of solids concentration $L(1-\epsilon)$, which have been

obtained for glass beads with three different intensity distributions of the x-ray source. The intensity distribution was varied by changing the target voltage V_0 applied to the x-ray tube and by using a 4,5 mm aluminum filter to harden radiation.

The three different calibration functions also indicate the operative range of the tomographic system. In order to measure low solids concentrations with an optimum of accuracy for a given length L the target voltage V_0 applied to the x-ray tube should be the minimum possible without using any filter. In our case with a maximum tube diameter of 0.19 m average solids concentrations $(1-\epsilon)$ from almost 0 up to 3 Vol-% can be detected with 35 keV applied. Such concentrations are typical for the downflow of a circulating fluidized bed.

The target voltage V_0 should be increased and radiation should be filtered to measure highest concentrations which usually can be found at the bottom of a circulating fluidized bed. With a target voltage of 60 keV and a 4.5 mm aluminum filter it is possible to use the system for average solids concentrations up to 20 Vol-% in a 0.19 m tube. However, the problem of applying higher voltage is that accuracy for low concentrations is worse and using filters measuring time increases because of lower radiation intensities.

After an adequate calibration it is possible to calculate the integral value of solids concentration $L(1-\epsilon)$ for each approximately linear beam. To calculate local solids concentrations inside the tube it is necessary to know many integral values $L(1-\epsilon)$ for a number of different directions. The calculation of local values of solids concentration $(1-\epsilon)$ is carried out by an Algebraic Reconstruction Technique (ART), which is an iterative algorithm to solve underdetermined linear equation systems. For industrial applications ART is rather used than e.g. Fourier inversion or convolutional backprojection, because it shows better results with limited data and it is very easy to incorporate prior knowledge like restrictions in the reconstruction area [6].

Due to the statistic nature of the generation of x-rays a minimum recording time at each direction is necessary to achieve a given accuracy of the solids concentration. As a consequence, only time averaged solids concentrations can be obtained. One solids concentration profile needs about 20 to 40 minutes to be measured, depending on solids concentration inside the tube.

However, the main advantage of this technique is the non-intrusive measurement of local solids concentrations even near to the wall of the tube, where other systems like intrusive probes deliver no reliable results because of their large measurement volumes. In addition to that, the spatial resolution of the system is relatively high. The system presented in this paper allows a minimum spatial resolution of 0.2 mm. Finally x-ray

computer tomography is insensitive to electronic charging of the gas-solids flow inside the circulating fluidized, which normally is a great problem especially for very fast measuring techniques like capacitance probes or electrical impedance tomography.

To prove the reliability of the whole tomographic system a cylinder of glass beads covered by an extremely thin layer of latex has been measured (shown in Figure 7). The mean solids concentration $(1-\epsilon)_{av}$ was calculated as 59.2 Vol-%. This academic object was measured with the same parameter of the x-ray tomography system like the results presented later on. After the reconstruction process the solids concentration distribution of the object was averaged to 61.2 Vol-%. The thin lines outside the cylinder of glass beads are caused by the ART-algorithm and called artifacts.

Also other experiments with objects of a certain solids concentration distribution show that the relative divergence between the given and the measured value of average solids concentration is maximum 5 %. However, the error of local solids concentration may be up to 10%.

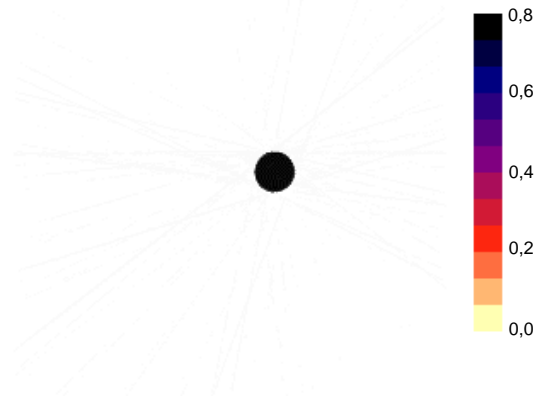


Figure 7: Reconstruction of a test object made of glass beads

3. EXPERIMENTAL SETUP

The x-ray computer tomography system has been installed at two different kinds of circulating fluidized beds. One plant was built up to investigate the upflow of a circulating fluidized bed with high solids concentrations inside. For the gas-solids flow is moving against the direction of gravity this reactor is called riser. The other plant is used to explain phenomena of the downflow part of a circulating bed and therefore it is termed downer.

Both plants shown in Figure 8 are special constructions of circulating fluidized beds. To realize a circulating gas-solids flow air is provided by a blower and mixed with solids at the bottom of the plants. Both phases flow against the

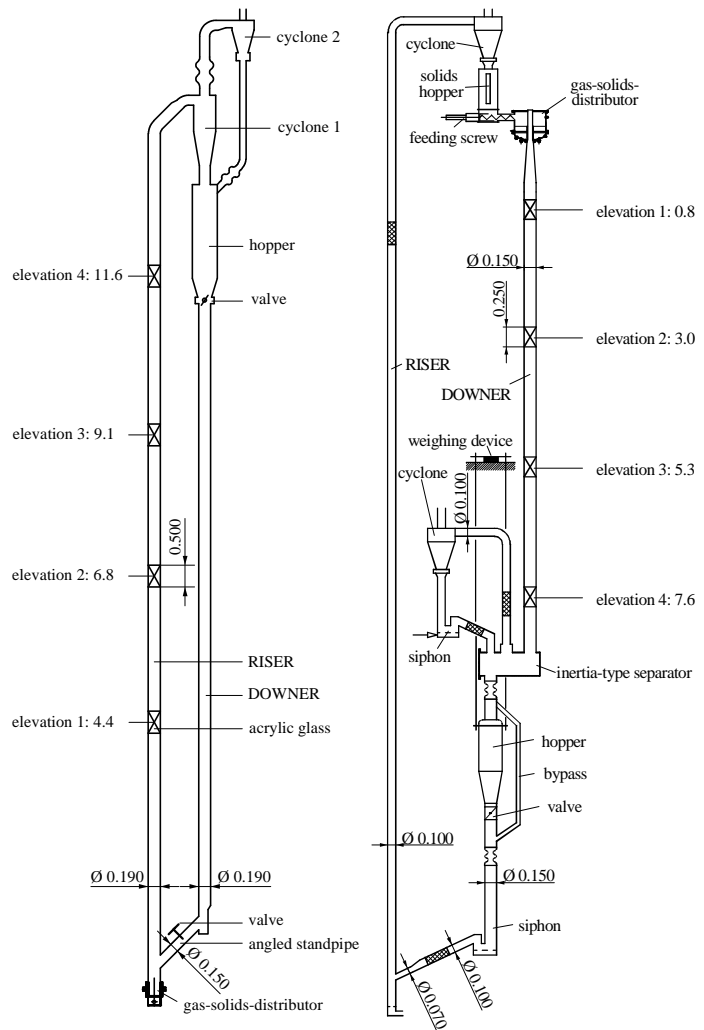


Figure 8: Sketch of the riser and downer plant

direction of gravity, vertically upwards. At the end of the upflow tube both phases are quickly and completely separated in cyclones. Segregated solids move downwards through the downer and then through an angled standpipe back into the riser. The gas flow rate through the circulating fluidized beds is measured by orifice meters. At each plants a number of differential pressure transducers are mounted to observe static pressure. The solid flux circulating in the plant can be measured by closing a valve below a hopper and weighing the variation of solid accumulation inside the hopper. In the riser plant the hopper is inserted at the top of the downflow whereas in the downer plant it is mounted close to the bottom. The main differences between both plants are the position of the gas-solids distributor and the additional solids segregation at the bottom of the downer plant. The riser plant consists of tube elements made of stainless steel with an inner diameter of 0.19 m and a total height of 14 m for the upflow. The downflow of the plant is as well made of stainless steel with an inner diameter of 0.15 m and 8.5 m total height.

In order to measure the solids distribution inside both plants with the tomographic system four 0.5 m respectively 0.25 m long plexiglas tube elements are inserted between the stainless steel elements. With plexiglas tube elements instead of stainless steel elements the decrease in intensity only because of tube material is reduced.

Experiments have been carried out with narrowly size distributed glass beads between 50 and 70 μm , which are ideal spherical and insensitive to breakage and attrition. The riser was operated at superficial gas velocities U_G from 2 to 7 m/s, which leads to solids circulating mass fluxes G_S from 30 up to 600 $\text{kg}/(\text{m}^2\text{s})$ and area weighted solids concentrations $(1-\varepsilon)_{av.}$ of 1.8 to 17.2 Vol-%. In the downer it is possible to adjust U_G between 0 and 7 m/s so that G_S from 30 up to 100 $\text{kg}/(\text{m}^2\text{s})$ and $(1-\varepsilon)_{av.}$ between 0.2 and 2.0 Vol-% can be obtained.

4. RESULTS AND DISCUSSION

For the results presented in the paper the radial concentration profiles are reconstructed from 128 angular projections to a 256 x 256 reconstruction grid according to a spatial resolution of 0.8 mm. At each angular position the x-ray linear detector is read out 200 times and the results are averaged. This implies an integration time of about 15 s for each of the 128 projections and in total a time of 30 minutes for one radial concentration profile. In Figure 9 and 10 the tube material shown as an intense black circle is not reconstructed together with solids but inserted afterwards because of different absorption coefficients for plexiglas and glass beads.

4.1. Riser plant

Figure 9 shows solids concentration distributions measured with the tomographic system at a superficial gas velocity U_G of 2.7 m/s and a specific mass flow rate G_S of 195 $\text{kg}/(\text{m}^2\text{s})$.

All three radial concentration profiles show a parabolic shape with a maximum concentration close to the wall and a minimum concentration in the center of the tube. This typical profile for the upflow in a circulating fluidized leads to solids and gas moving downward in a layer near the wall [14]. The mean value of solids concentration $(1-\varepsilon)_{av.}$ over the whole cross section decreases from elevation 1 to elevation 4 (Figure 8), because of acceleration of gas and solids from the bottom to the top of the riser. At the bottom of the plant local solids concentrations up to 45 Vol-% are reached near the wall of the tube, which is close the minimum fluidization concentration. It is remarkable that the shape of the solids concentration distribution is similar for all elevations of the riser even at different superficial gas velocities and different circulating mass fluxes.

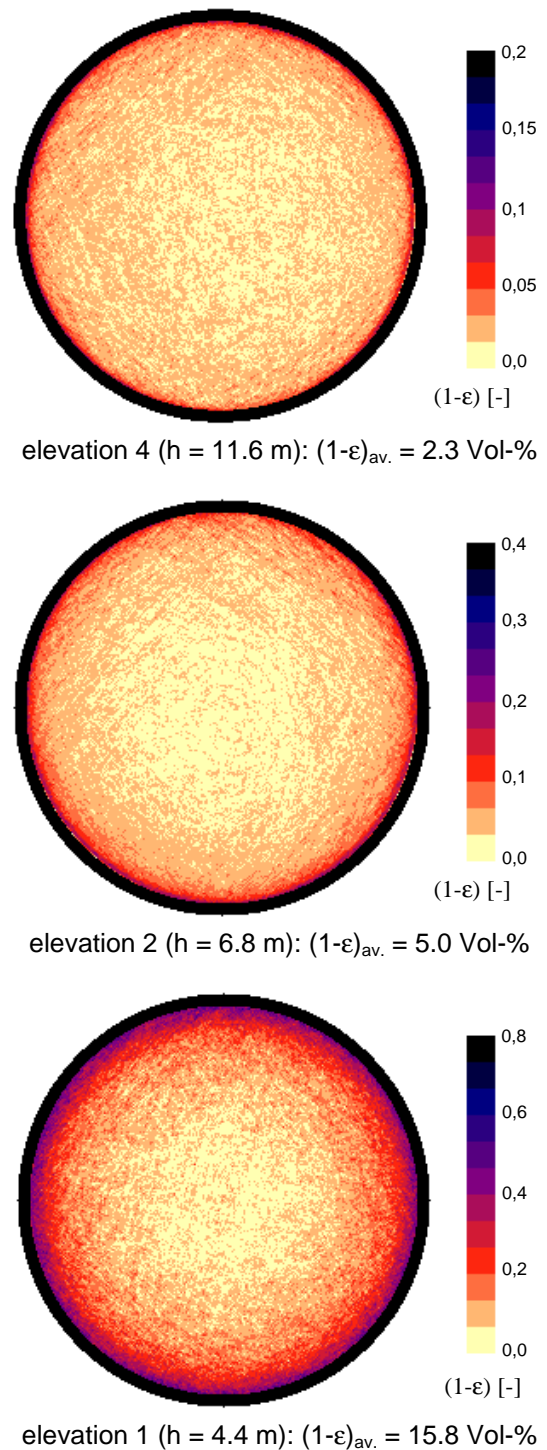
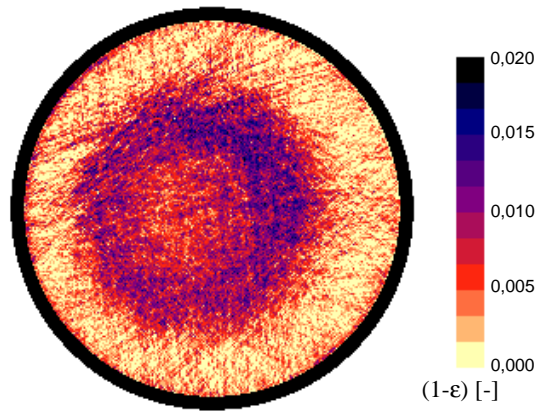


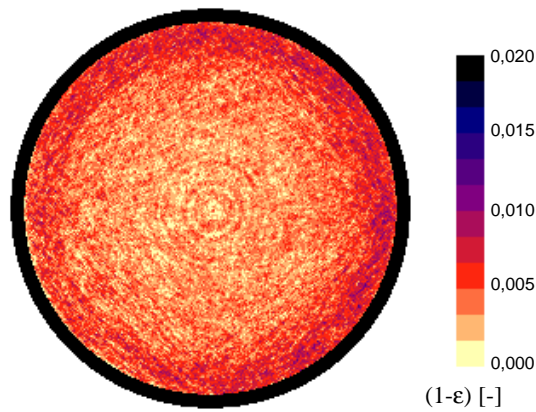
Figure 9: Solids concentration distribution in the riser ($U_G = 2.7 \text{ m/s}$, $G_S = 195 \text{ kg}/(\text{m}^2\text{s})$)

4.2. Downer plant

Following only one result of the downer plant shall be presented. Figure 10 shows radial solids concentration distributions obtained by the x-ray computer tomography system occurring at a superficial gas velocity U_G of 1.3 m/s and a circulating mass flux G_S of 45 $\text{kg}/(\text{m}^2\text{s})$.



elevation 2 (h = 3.0 m): $(1-\epsilon)_{av.} = 0.62$ Vol-%



elevation 3 (h = 5.3 m): $(1-\epsilon)_{av.} = 0.60$ Vol-%

Figure 10: Solids concentration distribution in the downer ($U_G = 1.3$ m/s, $G_S = 45$ kg/(m²s))

In comparison to the riser the height h of the downer is given as the distance from the gas-solids distributor, i.e. from the top of the downflow tube to the bottom. Comparing both solids concentration profiles in Figure 10 a rapid change in the flow structure for different elevations can be observed. At elevation 2, which is closer to the gas-solids distributor, most of the solids are concentrated in the center of the tube, whereas at elevation 3, which is 2.3 m downstream of elevation 2, an almost homogeneous solids concentration distribution is detected. This indicates a strong influence of the gas-solids distributor on the flow patterns inside a downer. Depending on the operating conditions of the gas-solids distributor at the top of the downer various solids concentration distributions can be observed, from a homogeneous distribution over a parabolic profile like in the riser to concentrated strands in the center of the tube.

More about flow structures of a downer can be found in [15].

5. CONCLUSIONS

An x-ray computer tomography system consisting of a 60 keV x-ray source and a linear x-ray detector has been developed to study flow structures of circulating fluidized bed. This system shows a lot of advantages in comparison to commonly used measuring techniques like capacitance or optical probes and electrical impedance tomography. Unlike intrusive probes x-ray computed tomography does not influence the flow structure inside the vertical tubes. Moreover this system is applicable even at higher temperatures or when electric charging caused by flowing particles occurs, because there is no contact to the measuring object.

In addition to that x-ray computer tomography allows a far higher spatial resolution than other systems. If that detailed local information should be obtained by probes a measuring time from 20 to 40 minutes, necessary for x-ray tomography, is relatively short. However, in comparison to electrical impedance tomography system this acquisition time is still orders of magnitude higher so that snapshots of the flow structure inside circulating fluidized beds are impossible to capture.

After calibrating the system it is possible, to measure average solids concentrations up to 20 Vol-% and a minimum spatial resolution of 0.2 mm. Testing the tomographic system with well defined objects shows that results are reliable within an error range of about 5 %.

Radial solids concentration profiles received both at the upflow and at the downflow of a circulating fluidized bed show the different hydrodynamic properties caused by the direction of gas-solids flow. This knowledge is essential for modeling chemical reactions inside such kind of reactors.

ACKNOWLEDGEMENT

Financial support of the experimental investigations by the *Deutsche Forschungsgemeinschaft (DFG)* is gratefully acknowledged.

NOTATION

c	velocity of light = $2.99792 \cdot 10^8$	m/s
e	electronic charge = $1.6022 \cdot 10^{-19}$	C
E	energy of x-ray	eV
g	gravitational acceleration = 9,80665	m ² /s
h	height of the riser facility	m
h	Planck's constant = $6.6262 \cdot 10^{-34}$	Js
I	x-ray intensity, transmission	-
I ₀	intensity of the x-ray source	-
L	thickness of absorbing material	m
G _S	specific solids mass flux	kg/(m ² s)
s	coordinate along an x-ray beam	m
U _G	superficial gas velocity	m/s
V ₀	high voltage applied to the x-ray tube	V
Z	atomic number	-
ε	porosity	-
1-ε	solids volume fraction	-
λ	wavelength	m
λ ₀	cutoff wavelength	m
μ	linear absorption coefficient	1/m
ρ	density of material	kg/m ³

- [9] J. F. Mulligan, „*Introductory College Physics*“, McGraw-Hill Book Company, New York, 1985
- [10] W. Minder, A. Liechti, „*Röntgenphysik*“, Springer Verlag, Wien, 1955
- [11] E. Hering, „*Physik für Ingenieure*“, VDI-Verlag, Düsseldorf, 1992
- [12] H. Morneburg, (ed.), „*Bildgebende Systeme für die medizinische Diagnostik*“, Publicis MCD Verlag, München, 1995
- [13] J.H. Hubbell: „*XCOM: Photo Cross Section Database*“, <http://www.physics.nist.gov>
- [14] F. Berruti, J. Chaouki, L. Godfroy, T.S. Pugsley, G.S. Patience, „*Hydrodynamics of Circulating Fluidized Bed Risers: A Review*“, Can. J. Chem. Eng. 73 (1995), pp. 579-602
- [15] P. Lehner, K.-E. Wirth, „*Effects of the gas/solids distributor on the local and overall solids distribution in a downer reactor*“, to be published in: CJChE special issue (1999)

REFERENCES

- [1] J.R. Grace, A.A. Avidan, T.M. Knowlton, „*Circulating Fluidized Beds*“, Blackie Academic & Professional, London, 1997
- [2] A.S. Issangya, D. Rai, J.R. Grace, K.S. Lim, „*Flow Behavior in the Riser of a High-Density Circulating Fluidized Bed*“, AIChE Symposium Series No. 317, Vol. 93 (1998), pp. 25-30
- [3] M.G. Schnitzlein and H. Weinstein, „*Design Parameters Determining Solid Hold-up in Fast Fluidized Bed System*“, in „*Circulating Fluidized Bed Technology II*“, Basu, P., Large, J.F. (eds.), Pergamon Press, New York, 1988, pp. 205-211
- [4] J. Chaouki, F. Larachi, M.P. Dudukovic (eds.), „*Non-Invasive Monitoring of Multi-phase Flows*“, Elsevier, Amsterdam, 1997
- [5] D.M. Scott and R.A. Williams (eds.), „*Frontiers in Industrial Process Tomography*“, Engineering Foundation, New-York, 1996
- [6] R.A. Williams and C.-G. Xie, „*Tomographic Techniques for Characterizing Particulate Processes*“, Part. Part. Syst. Charact. 10 (1993), pp. 252-261
- [7] R. Gordon, „*A Tutorial on ART*“, IEEE Transactions on Nuclear Science 21 (1974), pp. 78-93
- [8] G.T. Herman, A. Lent, S.W. Rowland, „*ART: Mathematics and Applications*“, J. theor. Biol. 42 (1973), pp. 1-32